analytical chemistry

ARTICLE

pubs.acs.org/ac

Deployment of a Carbon Isotope Ratiometer for the Monitoring of CO_2 Sequestration Leakage

Ian McAlexander,[†] Greg H. Rau,[‡] Jimmy Liem,[†] Thomas Owano,[†] Ray Fellers,[†] Douglas Baer,[†] and Manish Gupta*[,†]

[†]Los Gatos Research, 67 East Evelyn Avenue, Suite 3, Mountain View, California 94041, United States

[‡]Institute of Marine Sciences, University of California Santa Cruz, Santa Cruz, California 95064, United States

ABSTRACT: In an effort to monitor leakage from underground CO_2 storage, a field-deployable analyzer capable of rapidly measuring the CO_2 mixing ratio and $\delta^{13}C$ values ($\pm$0.05 ppm_v $\pm$ 0.2‰, 60 s) was deployed to distinguish between biogenic and fossil CO_2 sources. The analyzer was interfaced with a multiport inlet unit to allow autonomous sampling from multiple locations. The instrument and inlet interface were deployed at the Zero Emissions Research and Technology (ZERT) site (Bozeman, Montana, July 14−22, 2009) during a controlled, subsurface release of CO_2 depleted in ^{13}C. A biogenic diurnal cycle was observed far from the release, and the associated Keeling plot suggested a CO_2 source ($\delta^{13}C = -27.0 \pm 0.5$‰) consistent with local C_3 vegetation. Inlets near the leak showed large CO_2 mixing ratios (388/>40 000 ppm_v) whose predominant source was the release CO_2 (inferred $\delta^{13}C = -58.2 \pm 0.7$‰). Measurements 3 m from the source showed diurnal CO_2 cycles (382−2400 ppm_v) influenced by leaked CO_2, possibly due to diel air mixing. Finally, the data from all of the sampling inlets was combined to spatially localize the leak position.

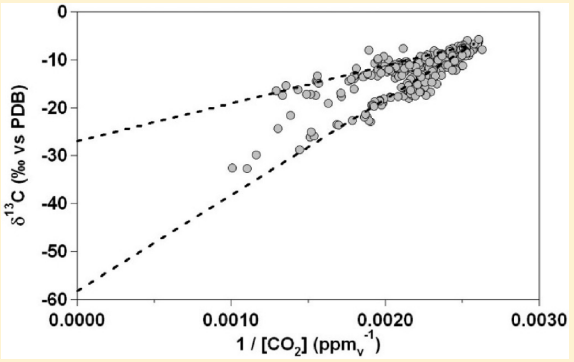

Anthropogenic carbon dioxide emissions are impacting earth's climate and ocean chemistry.[1] A variety of methods have been proposed to mitigate these effects, including capturing and storing CO_2 emissions.[2] Geological carbon sequestration (GCS) allows final storage of the captured and purified gas in geologic formations (e.g., oil or gas reservoirs, saline aquifers, and coal seams) that can potentially store the CO_2 indefinitely.[3]

One of the chief concerns regarding GCS is the potential for leakage of the stored CO_2 through boreholes, faults, or permeable rock formations.[3,4] Despite initial work suggesting that leakage rates are small,[5] there is not extensive data on long-term sequestration or large-volume injections, and careful monitoring of stored CO_2 is essential to demonstrate the efficacy of GCS. A variety of techniques are being developed to measure CO_2 leaking from GCS sites,[6,7] including chamber-based, eddy flux, tracer, and soil gas methods. Chamber methods involve placing an enclosure over the suspected leakage area and measuring CO_2 accumulation.[8] They are well-suited for small leaks; however, they alter the micrometeorology of the enclosed volume and are limited by spatial heterogeneity within the leakage area. Eddy flux methods involve using a fast CO_2 analyzer (e.g., 10−20 Hz), correlating the measurements to wind speed and direction, and determining the net CO_2 leakage flux coming from a large area.[9,10] Both chamber and flux techniques have difficulties distinguishing between naturally generated CO_2 (e.g., soil and plant respiration) and GCS leakage, and a recent method has focused on examining O_2/CO_2 correlations to discern the two sources.[7] Tracer studies address this problem by spiking the sequestered CO_2 with SF_6, perfluorocarbons,[11] isotopes,[12,7] or other distinguishing material and measuring the tracer at the surface. Although such methods can provide an accurate measure of CO_2 leakage, they may be cost-prohibitive and require extensive measurement instrumentation that is not readily field deployable (e.g., mass spectrometers). Soil gas measurements look for accumulation of leaked CO_2 in the soil prior to its release into the atmosphere. Promising results have been obtained using both laser-based, fiber-optic[13] and nondispersive infrared[14] sensors. A complementary method is also being considered to measure the change in soil carbon concentration using inelastic neutron scattering.[15] However, to date, these techniques have been complicated, and the soil carbon depletion mechanisms are poorly understood.[6,7]

Since the sequestered CO_2 may have an isotope ratio that is substantially different from other ambient sources, such as biogenic CO_2 ($\delta^{13}C \sim -8$, -14, -26, and -52‰ vs PDB for ambient air, C_4 vegetation, C_3 vegetation, and natural gas combustion products, respectively), a measurement of CO_2 isotope ratio versus the inverse of the CO_2 concentration (e.g., 2 end-member Keeling Plot) can be used to detect leakage from a geological reservoir.[16,17] Simulations have shown that leaks resulting in an increase of only a few parts per million volume in CO_2 may be discerned by a shift in the carbon isotope ratio.[6]

Received: March 28, 2011
Accepted: July 9, 2011
Published: July 09, 2011

Until recently, one limitation in implementing this technique was the lack of field-deployable instrumentation capable of accurately measuring the carbon isotope ratio of ambient CO_2. Laser-based isotope analyzers have addressed this issue,[18,19,7,20] and these technologies are now poised to be field-deployed for carbon sequestration studies.

In this study, we describe the deployment of a laser-based analyzer capable of making rapid (1 Hz) measurement of CO_2 concentration to better than ± 0.05 ppm_v (1σ in 60 s) and $\delta^{13}C$ to within $\pm 0.2‰$ (1σ in 60 s) at ambient levels (350−1000 ppm_v). Subsequent to the instrument fabrication and laboratory testing, it was interfaced to a multiport inlet unit and deployed for over 7 days at the Zero Emissions Research and Technology (ZERT) site during a controlled subsurface CO_2 leakage event. The analyzer could readily distinguish between biogenic and anthropogenic CO_2 and spatially localize the leakage.

Simultaneous to this study, another laser-based CO_2 isotope analyzer (Picarro WS-CRDS analyzer) was deployed at the same site[20] and manually manipulated across the leak location at 1−2 m/s. The instrument and data presented here differ from this concurrent measurement in several respects. Foremost, the Picarro analyzer does not measure the $^{12}CO_2$ and $^{13}CO_2$ concentrations simultaneously. Thus, for situations in which the CO_2 concentration varies rapidly (e.g., manually traversing a CO_2 leak and changes in wind direction), the instrument provides inaccurate readings that must be discarded.[20] Even after this extensive data filtering, this effect led to substantial scatter in the Keeling plots and false positives in the spatial localization of the leak (see Figures 3 and 4 in ref 20). The instrument presented below makes simultaneous measurements of $^{12}CO_2$ and $^{13}CO_2$ in a single laser sweep (e.g., ∼0.003 s), providing highly accurate data despite rapidly changing CO_2 concentrations. In addition, CO_2 concentrations and carbon isotope ratios are presented as a function of time, showing diurnal cycling and diel air mixing. Finally, the system was interfaced to an automated multiport inlet, enabling reproducible measurements at specific locations and periodic calibration.

METHODS

Off-Axis ICOS Carbon Dioxide Isotope Analyzer. The concentration and isotope ratio of ambient carbon dioxide are conventionally measured using nondispersive infrared spectroscopy and isotope ratio mass spectrometry, respectively. Although the former technology is readily field-deployable and widely implemented, the latter method is restricted to laboratory usage. In this study, we have utilized a Los Gatos Research CO_2 Isotope Analyzer that exploits a laser-based analytical method termed off-axis integrated cavity output spectroscopy (off-axis ICOS) to simultaneously measure both CO_2 concentration and carbon isotope ratio. The technique has been described elsewhere,[21] and only a brief overview will be provided below. A temperature-controlled DFB diode laser operating near 2.05 μm was coupled into a 59-cm-long, high-finesse optical cavity consisting of two highly reflective mirrors ($R \sim 0.99980$ as determined by cavity ringdown spectroscopy[22]) that provided an effective optical path length of 3 km. Light transmitting through the cavity was focused onto a thermoelectrically cooled x-InGaAs detector whose signal is passed through a high-gain, low-noise amplifier. A diaphragm pump continuously flowed gas through the cavity at 0.5 L/min, and a proportional solenoid valve retained the pressure inside the cavity to 38 Torr, assuring good absorption peak contrast. The gas temperature was regulated to 45 °C using a resistive heater and feedback control system.

The laser frequency was repeatedly tuned over 20 GHz to span over a $^{12}CO_2$ and $^{13}CO_2$ molecular absorption feature. Each scan required 3.3 ms (e.g., 300 Hz laser tuning), and 270−1350 transmission spectra (1 - 5 s) were averaged to achieve sufficient signal-to-noise ratio on the $^{13}CO_2$ absorption feature. The spectra were fit in real time to two Voigt profiles, and the absolute concentrations of $^{12}CO_2$ and $^{13}CO_2$ in the gas sample were determined from the integrated peak areas, gas temperature, effective optical path length, and measurement pressure in accordance with Beer's Law. The entire system was packaged into an enclosure, and a comprehensive software package was developed to control the instrument, save data, and autonomously sample multiple inlets and calibration gases. The instrument, calibration gases, and multiport inlet unit were all housed in an unregulated mobile laboratory to isolate them from precipitation and debris. Local 120 VAC power was provided at the deployment site.

Multiport Inlet Unit (MIU). The off-axis ICOS carbon dioxide isotope analyzer was interfaced to a custom multiport inlet unit to provide sampling from multiple locations along the leakage site (Figure 1). The MIU consisted of an array of electronic solenoid valves that allowed for the 15 inlets (13 sample and 2 calibration gas inlets) to be individually routed to the gas outlet via an applied digital signal. To minimize the time response of the measurement along the long sample lines, gas flowed continuously at 1 L/min through each sample inlet to the MIU using an additional diaphragm pump. The gas outlet was passed through a Nafion filter to dry the sample to <1000 ppm_v water prior to entering the analyzer. Nafion is extensively used in carbon dioxide concentration and isotope monitoring due to its minimum effect on the measurements.[18] Although the humidity is not monitored, the error induced by water vapor dilution is <0.1% at 1000 ppm_v water vapor. The MIU was interfaced to the instrument to autonomously switch between sample inlets and reference gases, as described below.

Zero Emissions Research and Technology (ZERT) Site. The ZERT Center was established to study GCS via modeling efforts, laboratory experiments, and field studies. The latter includes a field site in Bozeman, Montana where controlled subsurface gas leaks were conducted for testing of CO_2 detection instrumentation over the past 3 years.[23]

The instrument was deployed at this ZERT site from 7/14/2009 to 7/22/2009. An ∼100-m-long porous tube was horizontally buried 1−3 m under the ground, and pure CO_2 was leaked at a rate of 200 kg/day from 7/15/2009 to 8/15/2009 to simulate the expected leakage for a realistic GCS project (e.g., 200 Tg storage, 0.01% leakage per year, over a 70 000 m^2 fault results in ∼1 kg m^{-2} day^{-1}). The MIU inlets were configured as shown in Figure 1. Inlets A, C, D, F, H, and I were mounted 4 cm above the ground and spaced at 0.5 m intervals in a transect across the horizontal leak. Inlets E and J were spaced 1.5 m from inlets D and I, respectively, and inlets B and G were located 26 cm above inlets A and F, respectively. Inlet K was collocated with another measurement site approximately 2.8 m from the leakage site. Inlets L and M were located 50 m away from the site near the mobile laboratory and mounted 64 cm above the ground to serve as background control measurements. The actual CO_2 leak line was centered between inlets F and H. All of the inlets were connected to the MIU using 0.8 cm i.d. Teflon tubing to obtain sufficient gas conductance.

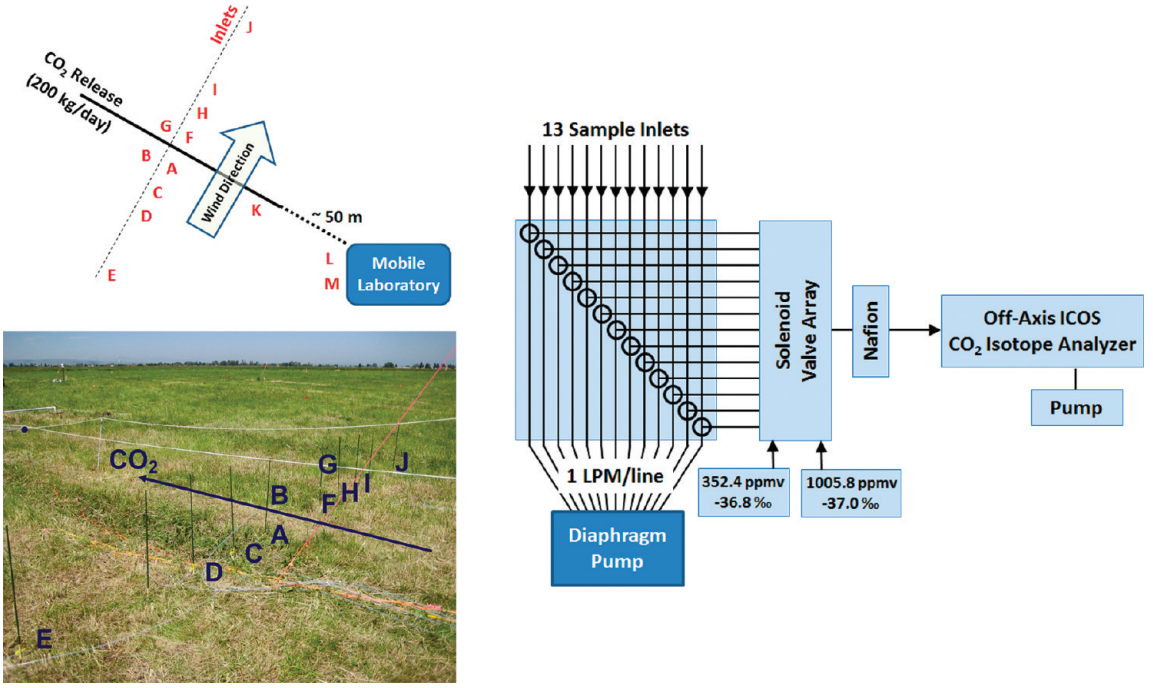

Figure 1. Ambient air was sampled from 13 gas inlets via 0.8 cm i.d. Teflon tubing (left) at a continuous rate of 1 LPM/line. Inlets A−J transected the CO_2 release as described in the text. Inlet K was collocated with another measurement team ~1 m from the leak. Inlets L and M were located near the mobile laboratory, 50 m from the release. The inlet lines and 2 certified calibration cylinders were all routed into a solenoid valve array, through a Nafion drying filter, and into the off-axis ICOS CO_2 isotope analyzer (right). The entire system was automated to cycle through the inlets every 35.5 min.

Several of the gas inlets (F, H, I, L, and M) were reconfigured during the run to assess the effects of sampling at different heights. The different sampling configurations and their relation to micrometeorological parameters will be examined in another study; however, in general, the prevailing wind direction blew from inlet E to J.

Measurement Sequence and Calibration Procedure. The MIU was operated to measure inlets A−M for 150 s/each. The first 50 s of data were discarded to ensure minimal sample crossover in the sampling lines, and the last 100 s of data was measured at 1 Hz prior to the release and 0.2 Hz during the release. Subsequent to quantifying the samples, two CO_2 reference tanks were measured for 90 s/each, and the last 60 s of data was retained. The first reference tank had a CO_2 concentration and carbon isotope ratio of 352.4 ± 0.5 ppm_v and −36.8 ± 0.2‰ vs PDB,[24] respectively, and the second reference tank had a CO_2 concentration and carbon isotope ratio of 1005.8 ± 0.5 ppm_v and −37.0 ± 0.2‰, respectively. These values were chosen to span the anticipated measurement range. The entire measurement sequence involved sampling 15 inlets and required 35.5 min.

The calibration gases were used to determine linear correction factors for the absolute concentrations of $^{12}CO_2$ and $^{13}CO_2$ and account for measurement drift. These factors were interpolated between calibration intervals to correct the measured data. The calibration procedure was extensively verified in laboratory studies,[25] and the correction was valid for CO_2 concentrations ranging from 350 to 1000 ppm_v. Note that a wide dynamic range is critical for GCS leak studies, where the measured CO_2 varies dramatically as shown below.

RESULTS AND DISCUSSION

Instrument Characterization. Prior to deploying the instrument in the field, extensive laboratory testing was undertaken to determine its analytical parameters. The instrument accuracy for $[CO_2]$ and $\delta^{13}C$ was determined to be better than ±0.05 ppm_v and ±0.2‰, respectively, by measuring 4 NOAA CMDL certified gas cylinders containing $[CO_2]$ and $\delta^{13}C$ ranging from 378−944 ppm_v and −8.3 to −23.8‰. The instrument calibration was further verified by measuring five independently characterized cylinders that ranged from $[CO_2]$ = 350 to 1000 ppm_v, and the measured results were within the samples' uncertainties (±0.5 ppm_v, ±1‰). Two of these cylinders were then deployed with the instrument to perform calibrations in the field. Note that the off-axis ICOS technology can readily address higher CO_2 concentrations (>3000 ppm_v) with appropriate reference gases,[25] but the calibration range was limited to 350−1000 ppm_v in this study.

The instrument precision was determined by measuring a constant CO_2 source (438 ppm_v, $\delta^{13}C$ = −9.7‰) for 18 h, and the resulting Allan deviation plot indicates short and long-term precisions of ±0.15‰ in 60 s and ±0.11‰ in 35 min. As noted above, 35.5 min was the 15 inlet cycle period in this study, and the instrument exhibits minimal drift over such a time interval, independent of ambient temperature fluctuations. Thus, no attempt was made to actively control the instrument temperature.

Finally, the time response of the instrument, which is primarily limited by the speed at which the laser stabilizes on the measured absorption transition, was determined to be <20 s by rapidly switching between two different samples. Thus, when switching between inlets, the first 50 s of data was discarded to ensure minimal transient behavior. As described above, transit time through the sample tubing was mitigated by continually flowing sample to the instrument, regardless of which inlet was being probed.

Deployment at the ZERT Site during a Controlled Subsurface Leak. The instrument was deployed continuously from

dx.doi.org/10.1021/ac2007834 |Anal. Chem. 2011, 83, 6223–6229

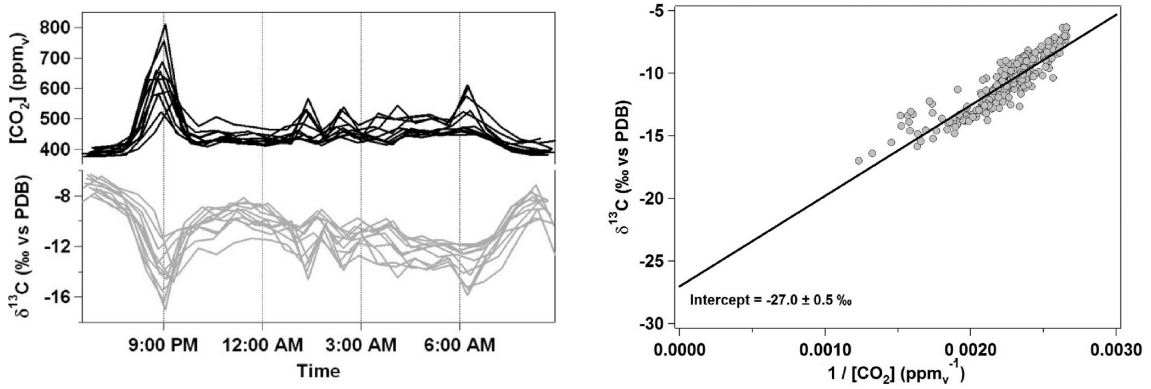

Figure 2. Measurements of ambient CO_2 concentrations (black) and carbon isotope ratios (gray) for inlets A−K prior to the CO_2 release (left). The measurements span 14 h and were taken from 7/14/2009 to 7/15/2009 at the ZERT site in Bozeman, Montana during light precipitation. The overlaid data traces show minimal spatial variation due to the delocalized carbon source (e.g., vegetation). A Keeling plot of the data (right) indicates that the carbon dioxide source that mixed with background air CO_2 during this period had an isotope ratio of $\delta^{13}C = -27.0 \pm 0.5‰$, which is consistent with that expected of biogenic CO_2, given the site's latitude[17] and C_3 vegetation.[6]

about 6 p.m. July 14 to 11 a.m. July 22, 2009. Prior to the CO_2 release, 18 h of ambient air measurements (Figure 2) showed background concentrations and isotope ratios ranging from 376 to 812 ppm_v and from −6 to −17‰, respectively. The resulting Keeling plot's *y* intercept indicates a carbon isotope source with $\delta^{13}C = -27.0 \pm 0.5‰$, which is consistent with a biogenic source, considering the site's latitude[17] and C_3 vegetation.[6] Note that the uncertainty in the Keeling plot intercept is primarily due to natural variability. The measurements were taken following a light rain, and elevated biogenic CO_2 levels (380−800 ppm_v) were observed relative to the dry conditions experienced during the rest of the experiment (<600 ppm_v). As expected, these measured values were comparable among sampling positions, since the biogenic carbon source (e.g., grass vegetation) was relatively uniformly distributed across the site.

On 7/15/10 at 12 p.m., subsurface ^{13}C-depleted CO_2 was released at a rate of 200 kg/day. The measured data and associated Keeling plots are shown in Figure 3 for four representative sample inlets that are distant (M), proximate (J, D), and very near (H) to the release.

Inlet M was far from the CO_2 release and was primarily influenced by biogenic CO_2, even during the gas release (Figure 3, top panel). The ambient CO_2 concentration varied between 361 and 539 ppm_v and shows a distinct diurnal pattern. The associated Keeling plot suggests that the CO_2 source has a carbon isotope ratio of $\delta^{13}C = -28.4 \pm 0.4‰$, slightly more depleted than the measurement made before the release. This observation may be due to natural variability[26] associated with meteorological parameters (e.g., rainfall, temperature); however, there may have been a small isotope shift due to mixing with the released gas.

Inlet H was located near the CO_2 release line and measured CO_2 values ranging from 388 to >40 000 ppm_v, well beyond the calibrated instrument range (Figure 3, second panel). At 11 a.m. on 7/17/2009, the inlet was moved from 4−5 to 15 cm above the ground to keep most of the readings within the calibration range. Excluding values above 1000 ppm_v, the associated Keeling plot indicates that the source CO_2 has an isotope ratio of $\delta^{13}C = -58.2 \pm 0.7‰$. The released CO_2 was obtained from a natural gas power plant. The same plant previously provided CO_2 to the ZERT site with a measured $\delta^{13}C \sim -52‰$ in 2007. In accordance with prior references,[7,20] we assume that the leaked CO_2 in this experiment has a comparable carbon isotope ratio, and the measured value of $\delta^{13}C = -58.2‰$ is consistent with the variability expected over such a long time frame. Note that samples of the leaked CO_2 were not provided to researchers, and thus, the actual isotope ratio is not well characterized.

Inlet J was located 3 m from the release and observed CO_2 concentrations ranging from 382 to 2400 ppm_v (Figure 3, third panel). After excluding CO_2 levels above 1000 ppm_v, the associated Keeling plot has an intercept of $\delta^{13}C = -53.0 \pm 0.5‰$, indicating that the majority of the nonbackground CO_2 comes from the released gas with minimal biogenic influence. However, the CO_2 concentration shows marked diurnal cycles similar to inlet M. One possible explanation for this observation is that, at night, the atmosphere is more stable, the leaked CO_2 remains close the ground, and the instrument measures elevated CO_2 concentrations with depleted carbon isotope ratios. During the day, convection rapidly dilutes the leaked CO_2 with background air, and the instrument measures CO_2 concentrations and isotope ratios commensurate with ambient air. Further modeling and correlations with meteorological parameters will be required to confirm this explanation.

Inlet D was located 1.5 m from the release and observed CO_2 values ranging from 380 to 994 ppm_v (Figure 3, bottom panel). Unlike the aforementioned data, the Keeling plot for inlet D shows contributions from background air and biogenic and released CO_2 in various mixing ratios. Note that the isotope ratio measurement can clearly distinguish between natural and leaked CO_2, even at levels that are well within the biogenic cycle (e.g., 350−500 ppm_v). The large distinction between the Keeling plots for the biogenic- (Figure 3, top panel) and leak- (Figure 3, second panel) influenced locations are indicative of the system changing from a two-source (e.g., air and vegetation) to three-source (e.g., air, vegetation, and leakage) mixing model.

The instrument provided CO_2 concentrations and isotope ratios at single sampling points (inlets A−M). To help localize the leak, the concentrations and isotope ratios between the inlets were linearly interpolated from the measured vales, as shown in Figure 4. The data were truncated to include only CO_2 concentrations lower than 1000 ppm_v. The location of the release (e.g., proximate to inlets F, H, and I) is clearly evident in the data. Similarly, the mixing of released and biogenic CO_2 is observed in the intermediate isotopic values occurring between −60‰ and −27‰. The data can be readily normalized for background CO_2

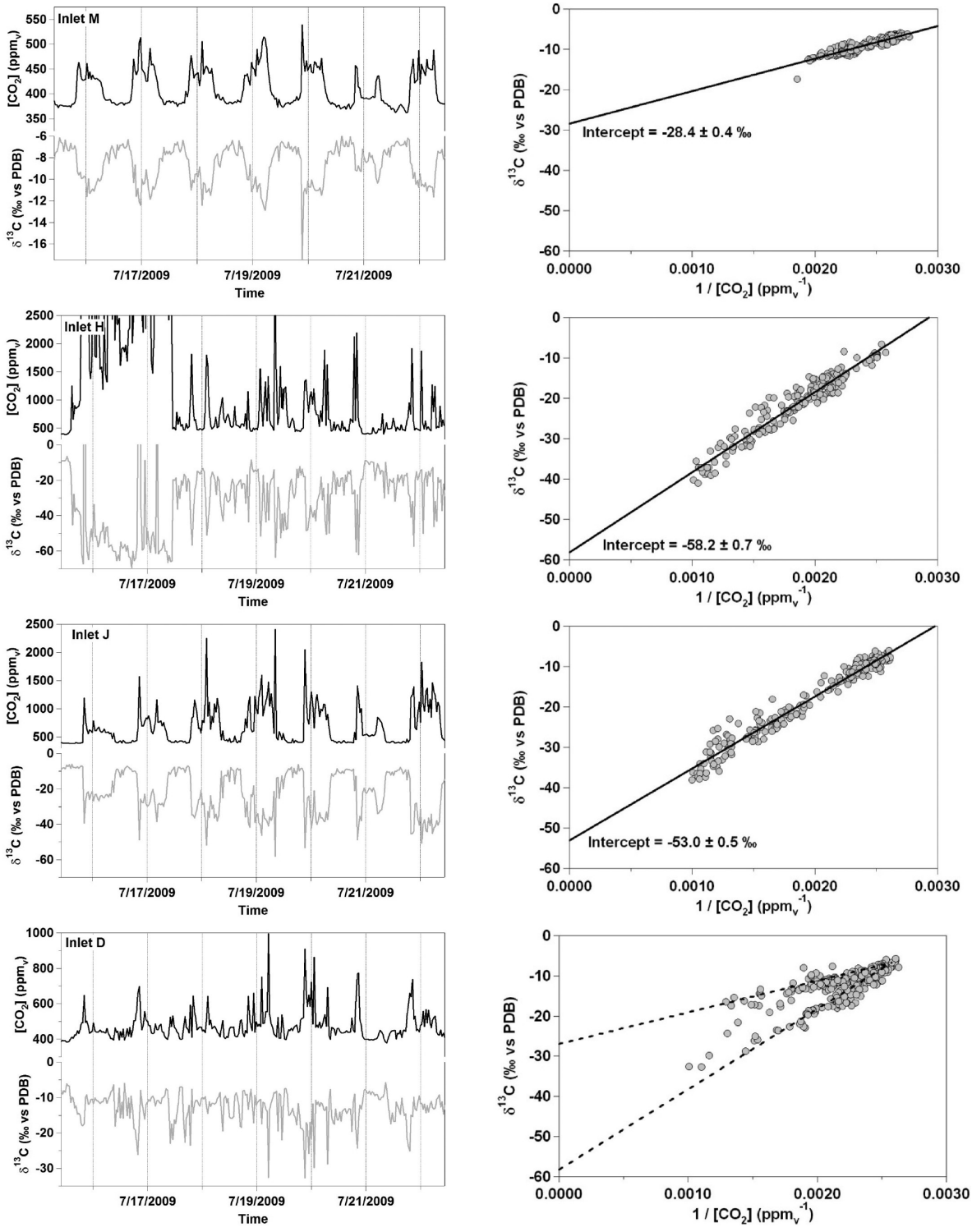

Figure 3. Measurements of ambient CO_2 concentrations (black) and carbon isotope ratios (gray) for inlets M, H, J, and D during the CO_2 release (left) and their associated Keeling plots (right). Inlet M was located 50 m from the release and shows diurnal cycling of biogenic CO_2 (top panel). Inlet H, which was repositioned during the experiment to avoid saturation, was located near the gas release and predominantly measures leaked CO_2 (second panel). Inlet J was located 3 m from the release, and the carbon isotope ratio indicates that the measured CO_2 was due to leak (third panel); however, the diurnal cycles in the measured CO_2 may be due to diel air mixing. Inlet D was located 1.5 m from the release, and the Keeling plot shows mixing between biogenic and released CO_2 (bottom panel). The dashed lines indicate the linear, 2-member mixing model for biogenic ($\delta^{13}C = -27‰$) and leaked ($\delta^{13}C = -58‰$) CO_2.

values by looking at inlets that are far from the release (e.g., inlets L and M).

Identifying a GCS leak requires measuring an increase in CO_2 concentration and observing a discernible shift in $\delta^{13}C$ outside of

dx.doi.org/10.1021/ac2007834 |*Anal. Chem.* 2011, 83, 6223–6229

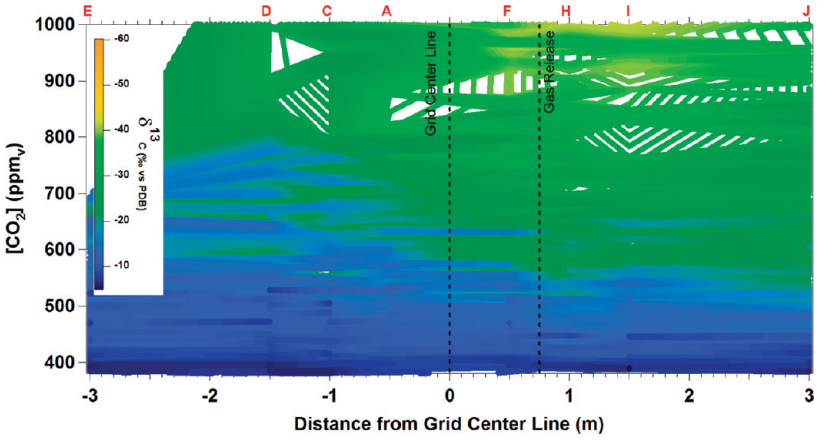

Figure 4. Interpolated color contour plot indicating CO_2 concentration and carbon isotope ratio as a function of distance from the CO_2 release. The data have been truncated to include only $[CO_2] < 1000$ ppm_v, and the inlet positions are indicated along the top axis relative to the release line. The location of the release is clearly evident by the increase in concentration and decrease in $\delta^{13}C$. Ambient CO_2 isotope ratios range from −8 to −20‰ at this site, and the leaked gas is substantially lighter. As indicated in Figure 1, the wind direction is from inlet E to inlet J.

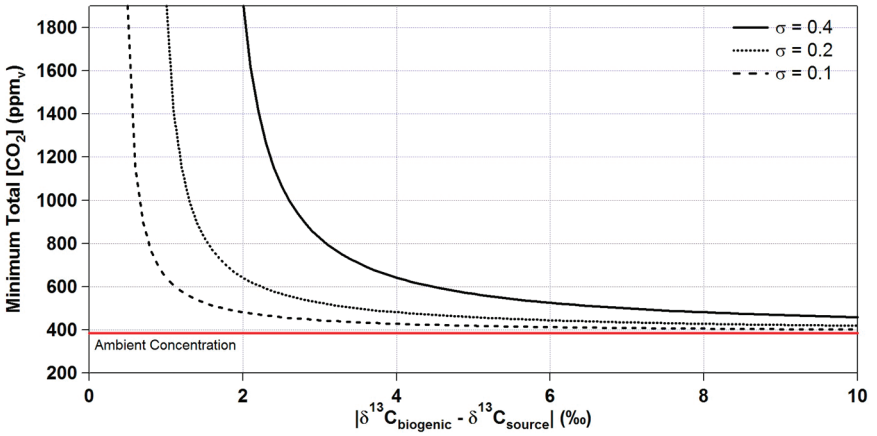

Figure 5. Minimum total CO_2 measurement needed to differentiate the presence of a CO_2 source from a biogenic CO_2 source when the absolute difference in $\delta^{13}C$ between source and biogenic CO_2 is known and the measurement precision (σ) of the $\delta^{13}C$ is as specified. The minimum CO_2 is determined by finding the CO_2 value when the Keeling plot of the source plus background air CO_2 mixing diverges by more than 4σ from the Keeling plot of the biogenic plus background air CO_2 mixing. The calculations assume an ambient CO_2 concentration of 385 ppm_v.

natural variability. The minimum detectable CO_2 can be determined by comparing the Keeling plot for air−biogenic mixing with that of air-leakage mixing. In a very simplistic analysis, when the CO_2 concentration at which the two $\delta^{13}C$ values differ by more than 4 times the measurement standard deviation (4σ), the instrument can be said to discern the leaked CO_2 from the biogenic source. Figure 5 shows the minimum detectable CO_2 versus the $\delta^{13}C$ difference between the biogenic and fossil sources for various measurement precisions. Note that such CO_2 threshold values will depend on the mean and variability of the fossil and biogenic CO_2 sources at a particular site as well as the measurement precision of the analytical instrument. This simple analysis assumes that the Keeling plots are the result of linear and well-behaved two-source mixing. A more complete analysis would require modeling of the source terms and their interplay with meteorological parameters.

Scaling up this measurement technique to address a realistic GCS site (~ 70 000 m^2), will require a much larger number of sampling inlets. Extrapolating from the data presented in Figure 4, the analyzer should be capable of detecting an upwind CO_2 leak at ~10−15 m from the leak location. Thus, the GCS site would have to be equipped with sampling inlets spaced at ~10 m, and each inlet would cover a 400 m^2 area. The entire site would then require ~175 inlets. Alternatively, the instrument could be deployed in a manner similar to the concurrent study[20] and traversed across the entire GCS site.

Future work will focus on using the data with other collocated measurements (e.g., wind speed and direction) to estimate the CO_2 leak rate. The biogenic signal will also be further analyzed to separate photosynthetic CO_2 uptake from respiration isotope effects. Finally, the analyzer can be coupled to chambers to measure very small gas fluxes or operated in a high-frequency (e.g., 10 Hz) mode to utilize the eddy flux technique.

AUTHOR INFORMATION

Corresponding Author

*E-mail: m.gupta@lgrinc.com.

■ ACKNOWLEDGMENT

We thank Laura Dobeck and Lee Spangler in the Department of Chemistry at Montana State University for their permission and assistance in deploying the instrument at the ZERT site during the CO_2 release experiment. We also acknowledge funding through the DOE SBIR program (Grant no. DE-FG02-06ER84606).

■ REFERENCES

(1) Parry, M. L., Canziani, O. F., Palutikof, J. P., van der Linden, P. J., Hanson, C. E., Eds.; *Contribution of Working Group II to the Fourth Assessment Report of the Intergovernmental Panel on Climate Change*; Cambridge University Press: New York, 2007.

(2) Metz, B., Davidson, O. R., Bosch, P. R., Dave, R., Meyer, L. A., Eds.; *Contribution of Working Group III to the Fourth Assessment Report of the Intergovernmental Panel on Climate Change*; Cambridge University Press: New York, 2007.

(3) Metz, B, Davidson, O. R., de Coninck, H., Loos, M., Meyer, L. A., Eds.; *Carbon Dioxide Capture and Storage: Special Report of the Intergovernmental Panel on Climate Change*; Cambridge University Press: New York, 2005.

(4) Pollak, M. F.; Wilson, E. J. *Environ. Sci. Technol.* **2009**, *43*, 3035–3041.

(5) Hovorka, S. D.; Benson, S. M.; Doughty, C.; Freifeld, B. M.; Sakurai, S.; Dailey, T. M.; Kharaka, Y. K.; Holtz, M. H.; Trautz, R. C.; Nance, S. H.; Myer, L. R.; Knauss, K. G. *Environ. Geosci.* **2006**, *13*, 105–121.

(6) Leuning, R.; Etheridge, D.; Luhar, A.; Dunse, B. *Int. J. Greenhouse Gas Control* **2008**, *2*, 401–414.

(7) Fessenden, J. E.; Clegg, S. M.; Rahn, A.; Humphries, S. D.; Baldridge, W. S. *Environ. Earth Sci.* **2010**, *60*, 325–334.

(8) Lewicki, J. L.; Oldenburg, C. M.; Dobeck, L.; Spangler, L. *Geophys. Res. Lett.* **2007**, *34*, L24402.

(9) Lewicki, J. L.; Hilley, G. E. *Geophys. Res. Lett.* **2009**, *36*, L21802.

(10) Lewicki, J. L.; Hilley, G. E.; Fischer, M. L.; Pan, L.; Oldenburg, C. M.; Dobeck, L.; Spangler, L. *J. Geophys. Res.* **2009**, *114*, D12302.

(11) Wells, A.; Strazisar, B.; Diehl, J. R.; Veloski, G. *Environ. Earth Sci.* **2010**, *60*, 299–305.

(12) Bachelor, P. P.; McIntyre, J. I.; Amonette, J. E.; Hayes, J. C.; Milbrath, B. D.; Saripalli, P. *J. Radioanal. Nucl. Chem.* **2008**, *277*, 85–89.

(13) Humphries, S. D.; Nehrir, A. R.; Keith, C. J.; Repasky, K. S.; Dobeck, L. M.; Carlsten, J. L.; Spangler, L. H. *Appl. Opt.* **2008**, *47*, 548–555.

(14) Lewicki, J. L.; Hilley, G. E.; Dobeck, L.; Spangler, L. *Environ. Earth Sci.* **2010**, *60*, 285–297.

(15) Wielopolski, L.; Mitra, S. *Environ. Earth. Sci.* **2010**, *60*, 307–312.

(16) Keeling, C. D. *Geochim. Cosmochim. Acta* **1961**, *24*, 277–329.

(17) Bakwin, P. S.; Tans, P. P.; White, J. W. C.; Andres, R. J. *Glob. Biogeochem. Cycles* **1998**, *12*, 555–562.

(18) Bowling, D. R.; Sargent, S. D.; Tanner, B. D.; Ehleringer, J. R. *Agric. Forest Meteorol.* **2003**, *118*, 1–19.

(19) Moyes, A. B.; Schauer, A. J.; Siegwolf, R. T.; Bowling, D. R. *Rapid Commun. Mass Spectrom.* **2010**, *24*, 894–900.

(20) Krevor, S.; Perrin, J.; Esposito, A.; Rella, C.; Benson, S. *Int. J. Greenhouse Gas Control* **2010**, *4*, 811–815.

(21) Baer, D. S.; Paul, J. B.; Gupta, M.; O'Keefe, A. *Appl. Phys. B: Laser Opt.* **2002**, *75*, 261–265.

(22) Deacon, D. A. G.; O'Keefe, A. *Rev. Sci. Instrum.* **1988**, *59*, 2544–2551.

(23) Spangler, L. H.; Dobeck, L. M.; Repasky, K. S.; Nehrir, A. R.; Humphries, S. D.; Barr, J. L.; Keith, C. J.; Shaw, J. A.; Rouse, J. H.; Cunningham, A. B.; Benson, S. M.; Oldenburg, C. M.; Lewicki, J. L.; Wells, A. W.; Diehl, J. R.; Strazisar, B. R.; Fessenden, J. E.; Rahn, T. A.; Amonette, J. E.; Barr, J. L.; Pickles, W. L.; Jacobson, J. D.; Silver, E. A.; Male, E. J.; Rauch, H. W.; Gullickson, K. S.; Trautz, R.; Kharaka, Y.; Birkholzer, J.; Wielopolski, L. *Environ. Earth Sci.* **2010**, *60*, 227–239.

(24) Note that all carbon isotope ratios presented in this paper are vs PDB, and all uncertainties are stated as 1σ.

(25) McAlexander, W. I.; Fellers, R.; Owano, T. G.; Baer, D. S. *Am. Geophys. Union Fall Meeting* **2010**, B23A–0386.

(26) Sun, W.; Resco, V.; Williams, D. G. *Oceologia* **2010**, *164*, 297–310.